



CT findings, prognosis, and follow-up of pulmonary artery periadventitial hematoma with aortic dissection: a retrospective single-center study

Hirofumi Koike[^], Eijun Sueyoshi, Chika Somagawa, Hiroki Nagayama, Ryo Toya

Department of Radiology, Nagasaki University Graduate School of Biomedical Sciences, Nagasaki University School of Medicine, Nagasaki, Japan

Contributions: (I) Conception and design: H Koike, E Sueyoshi; (II) Administrative support: R Toya; (III) Provision of study materials or patients: H Koike, C Somagawa, H Nagayama; (IV) Collection and assembly of data: C Somagawa; (V) Data analysis and interpretation: H Koike; (VI) Manuscript writing: All authors; (VII) Final approval of manuscript: All authors.

Correspondence to: Hirofumi Koike, MD. Department of Radiology, Nagasaki University Graduate School of Biomedical Sciences, Nagasaki University School of Medicine, 1-7-1 Sakamoto, Nagasaki 852-8501, Japan. Email: hkoike@nagasaki-u.ac.jp.

Background: Pulmonary artery periadventitial hematoma (PAPH) with aortic dissection (AD) is a rare condition but has been reported to correlate with prognosis. However, there are few cases of PAPH, and the relationship with computed tomography (CT) findings of AD are unknown. This study aimed to evaluate CT findings and early prognosis in patients with PAPH in AD.

Methods: This was a retrospective analysis of data from patients with Stanford type A AD diagnosed with contrast-enhanced CT in our institution from April 2008 to February 2023; 316 patients were included in the analyses. Patients comprised a PAPH group (n=78) and a non-PAPH group (n=238). The PAPH group was further divided into a group that died within 1 week of onset (death group; n=15) and a group that survived (alive group; n=63). PAPH was classified into three grades on the basis of the CT findings, as follows: Grade 1: PAPH only in the mediastinum; Grade 2: PAPH that extended into the lung field, with/without interlobular septa; and Grade 3: PAPH with pulmonary hemorrhage

Results: Compared with the non-PAPH group, the PAPH group had higher rates of early death (P=0.001), pericardial (P<0.001) and mediastinal hemorrhage (P<0.001). When comparing the death and alive groups, there was a significant difference in the rates of inoperable case (P<0.001), Grade 3 PAPH (PAPH with pulmonary hemorrhage) (P<0.001), and hemothorax (P=0.02). Multivariable analysis showed a significant association between Grade 3 PAPH (PAPH with pulmonary hemorrhage) and early death (P=0.004).

Conclusions: Standard type A AD with PAPH is not rare. Mortality was higher in the PAPH group *vs.* the non-PAPH group, and Grade 3 PAPH (PAPH with pulmonary hemorrhage) was a significant risk factor for early death.

Keywords: Pulmonary artery periadventitial hematoma (PAPH); aortic dissection (AD); prognosis; computed tomography (CT)

Submitted Dec 16, 2023. Accepted for publication Mar 01, 2024. Published online May 17, 2024.

doi: 10.21037/jtd-23-1914

View this article at: <https://dx.doi.org/10.21037/jtd-23-1914>

Introduction

Pulmonary artery periadventitial hematoma (PAPH) is a rare complication of Stanford type A aortic dissection (AD) (1-8).

Because the ascending aorta and pulmonary trunk have a common adventitia at the root of the great vessels (9), extravasated blood from the ascending aorta can extend

[^] ORCID: 0000-0001-9460-0928.

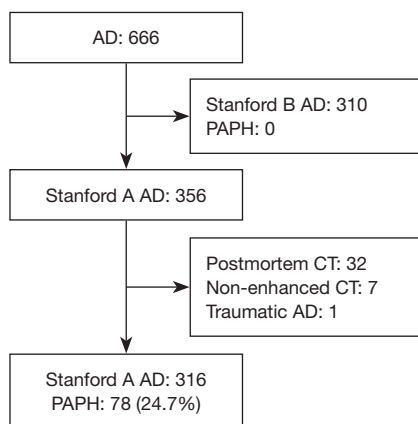


Figure 1 Flowchart showing the patient selection. AD, aortic dissection; PAPH, pulmonary artery periaortic hematoma; CT, computed tomography.

between the media and adventitia of the main pulmonary artery (PA). PAPH can cross the barrier of the pulmonary hilum, and dissect the bronchovascular sheaths and flow into the pulmonary interstitium (1-3,7). One study reported that PAPH with Stanford type A AD indicates a poor prognosis (10); however, there are few studies of PAPH. To the best of our knowledge, no studies have examined the long-term temporal evolution of PAPH, or patient characteristics and the relationship with computed tomography (CT) findings of AD between patients with *vs.* without PAPH.

The objective of the present study was to examine the long-term changes associated with PAPH, and differences in patient characteristics and the relationship with CT

findings of AD between patients with *vs.* without PAPH. We also investigated how patient characteristics and CT findings contributed to early prognosis in the PAPH group. We present this article in accordance with the STROBE reporting checklist (available at <https://jtd.amegroups.com/article/view/10.21037/jtd-23-1914/rc>).

Methods

Patient population

The study was conducted in accordance with the Declaration of Helsinki (as revised in 2013). This retrospective study was approved by the institutional review board of Nagasaki University Hospital (No. 23061912), and the institutional review board waived the need for written informed consent because of the retrospective study design. From April 2008 to February 2023, 666 consecutive patients were diagnosed as having AD on CT in our hospital for the first time. Among them, 310 patients had Stanford type B AD and no PAPH. The remaining 356 had Stanford type A AD and were ineligible to participate in this study if they had died before they underwent CT (postmortem CT), underwent only non-enhanced CT and not contrast-enhanced CT (CECT), or had traumatic AD. Therefore, 316 patients [151 men (47.8%) and 165 women (52.2%); mean age (standard deviation): 70.9 years (12.7)] were included in the final cohort (Figure 1). All of these patients were identified in a retrospective review of medical records performed at a single medical institution. Among the 316 patients, 78 patients (24.7%) had PAPH, and 238 patients (75.3%) had no PAPH on CECT. Patient death was defined as occurring within 1 week after the first CT, for the evaluation of early prognosis. As a result, the patients in the PAPH group were divided into a death group (n=15) and an alive group (n=63), and all surviving patients in the alive group were followed (mean 31.6±37.7 months) after they underwent the first CT.

CT imaging

For all patients with AD, CT studies were performed within 24 hours of onset and comprised non-enhanced CT and CECT in all patients. CT images were obtained using a helical technique with a 64-detector-row CT scanner (Somatom Definition or Definition Flash scanner; Siemens Medical Systems, Erlangen, Germany). Helical CT scans were obtained from the top of the thorax to

Highlight box

Key findings

- Pulmonary artery periaortic hematoma (PAPH) with Stanford type A aortic dissection (AD) is a risk factor for early death.

What is known and what is new?

- PAPH with Stanford type A AD sometimes occurs because the ascending aorta ruptures through the posterior aspect of the aortic root into the common adventitia of the aorta and pulmonary artery.
- Anatomically, high rates of pericardial and mediastinal hemorrhage may be associated with PAPH.

What is the implication, and what should change now?

- All patients with type A AD should be indicated for surgery. However, especially in patients with serious condition due to Grade 3 PAPH (PAPH with pulmonary hemorrhage), emergency surgery is essential to save lives.

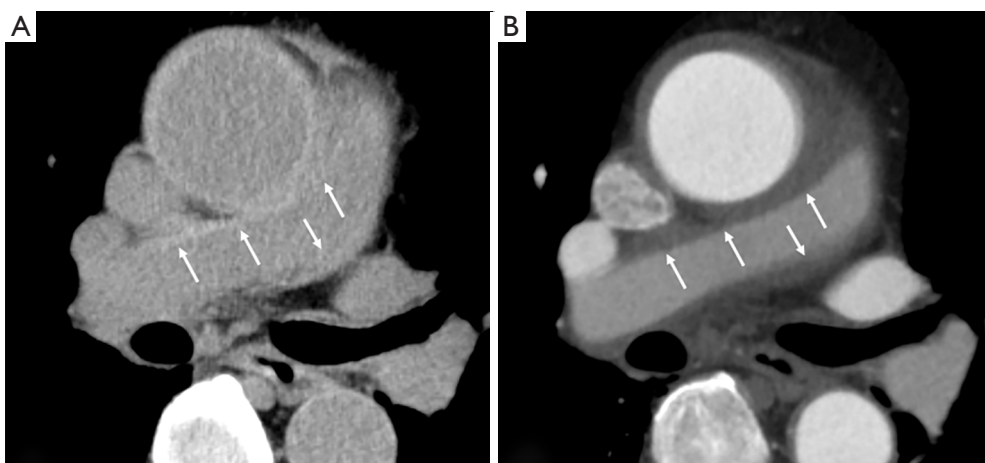


Figure 2 Images for a 76-year-old man with Grade 1 PAPH. (A) Non-enhanced CT showing a higher attenuation area than that of blood along the wall of the pulmonary trunk and right main PA (white arrows); (B) CECT showing no contrast enhancement within the area (white arrows). This was considered a hematoma due to PAPH. PAPH, pulmonary artery periaortic hematoma; CT, computed tomography; PA, pulmonary artery; CECT, contrast-enhanced CT.

the iliac artery. The scanning parameters were as follows: tube voltage: 100–120 kVp and tube current: 140–200 mAs (effective). Reconstruction was performed using a 2-mm slice thickness and 2-mm intervals. CECT was performed using a bolus intravenous injection of contrast media (Iopamidol 370; Bayer Yakuhin, Osaka) at 4.0 mL/s (total volume, 1 mL/kg) with a 20-mL saline chaser injection at 4.0 mL/s. CT data acquisition began at 20–30 s and 120–150 s (two phases) after the start of contrast material injection. Electrocardiographic gating was not used.

CT imaging analysis

CT images were retrospectively assessed by two experienced cardiovascular radiologists with 12 and 27 years, respectively, of experience reading cardiovascular CT images. The radiologists were unaware of the patients' clinical conditions and worked independently. Axial CT images (soft tissue window setting) and multiplanar reformatted (coronal and multiplanar sagittal) images were viewed, both of which had a slice thickness of 2.0 mm and a 2.0-mm slice interval. When different findings were obtained, final decisions were reached by consensus between the two radiologists.

The diagnosis of PAPH of the pulmonary trunk and/or a major PA was established on CT. First, a crescent-shaped or circumferential area along the wall of the PA with higher attenuation than that of the blood on non-enhanced CT was identified. Second, no contrast enhancement within the area on CECT was confirmed (*Figure 2*). Among the

316 patients with Stanford type A AD, CT images were evaluated by focusing on the following features: (I) false lumen: open or closed; and (II) complications: pericardial hemorrhage, mediastinal hemorrhage, and hemothorax. Moreover, among the 78 patients with PAPH, CT images were evaluated by focusing on the following features: (I) false lumen: open or closed; (II) complications: pericardial hemorrhage, mediastinal hemorrhage, and hemothorax; (III) presence of stenosis of the main PA due to PAPH. In this study, the presence of stenosis of the main PA was defined as stenosis greater than 25%; and (IV) extent of PAPH at the initial CT. We classified the extent of PAPH into three grades, as follows: (I) Grade 1: PAPH of the PA in only the mediastinum (*Figure 2*); (II) Grade 2: PAPH extending into the lung field with or without interlobular septa (*Figure 3*); and (III) Grade 3: PAPH with pulmonary hemorrhage, that is, blood extending into the alveoli beyond the tissue surrounding the PA (*Figure 4*).

Follow-up CECT was performed as needed by a cardiovascular surgeon in our hospital. We investigated these follow-up CT images and evaluated the changes in PAPH. We considered that a hematoma due to PAPH had disappeared if both areas along the wall of the PA had higher attenuation than that of blood on non-enhanced CT, and if the non-enhanced area on CECT had completely disappeared compared with the first non-enhanced CT and CECT (*Figure 5*). Moreover, we also assessed whether PA diameter changed during the follow-up after PAPH had disappeared. The same two cardiovascular radiologists

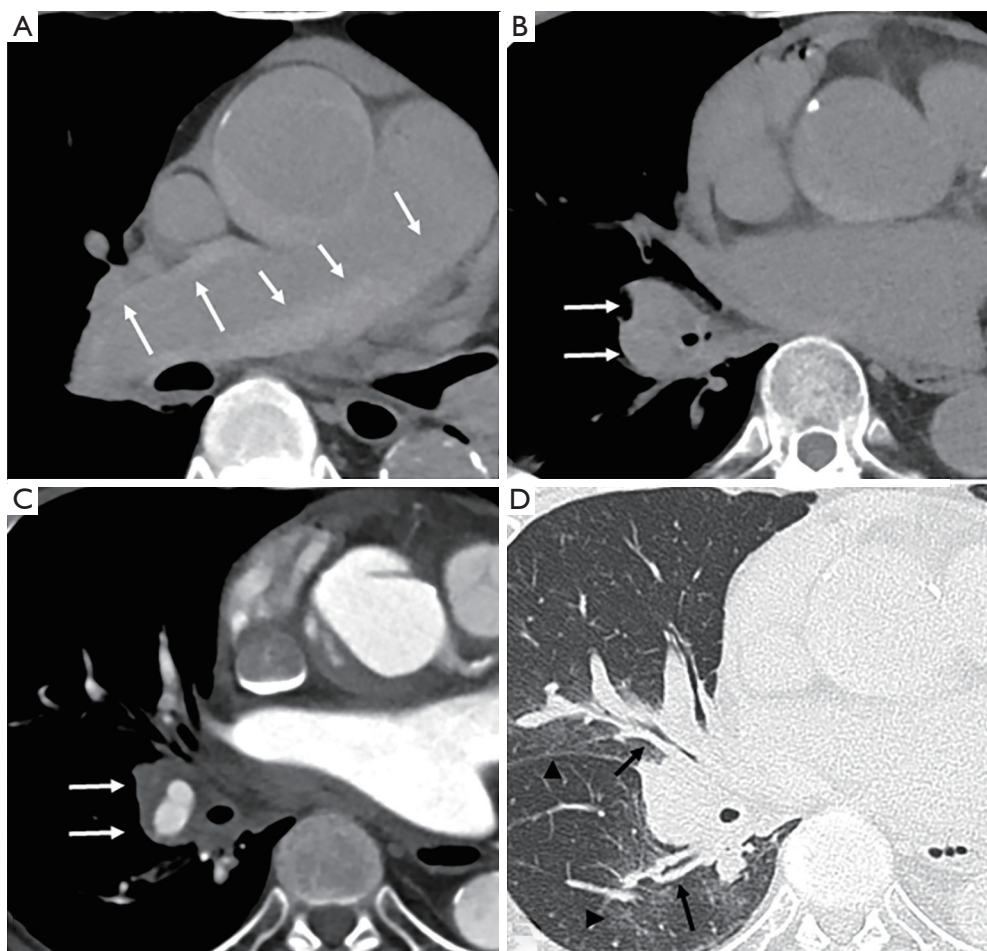


Figure 3 Images for a 91-year-old man with Grade 2 PAPH. (A) Non-enhanced CT showing a relatively thick higher attenuation area than that of blood along the wall of the pulmonary trunk and right main PA (white arrows); (B) non-enhanced CT showing a higher attenuation area than that of blood around the right PA in the right lung field (white arrows); (C) CECT showing no contrast enhancement within the area (white arrows), which was considered a hematoma due to PAPH; (D) CT (lung window setting) showing peribronchovascular interstitial thickening (black arrows) with faint ground-glass opacities (black arrowheads) in the right lung field, indicating peribronchovascular interstitial hemorrhage. PAPH, pulmonary artery periaortic hematoma; CT, computed tomography; PA, pulmonary artery; CECT, contrast-enhanced CT.

independently measured the maximum diameter of the main PA on the axial CECT (Figure 5D). The mean values of the maximum diameter of the main PA were used for analysis. We compared the size between the CT image when PAPH disappeared and the final CT image during the follow-up on the same slice image.

Statistical analysis

We used the D'Agostino-Pearson test to assess the normality of the data. We presented non-normally

distributed variables as the median and interquartile range. Continuous variables were presented as the mean \pm standard deviation, and categorical data were presented as counts and proportions. The patients' age was compared between the PAPH group and non-PAPH group, and between the death group and alive group using the Mann-Whitney *U* test. The maximum diameter of the main PA was compared between the CT images when PAPH disappeared and the final CT images during the follow-up using the Wilcoxon signed-rank test. The patients' characteristics and the CT findings were compared between the PAPH and non-PAPH groups,

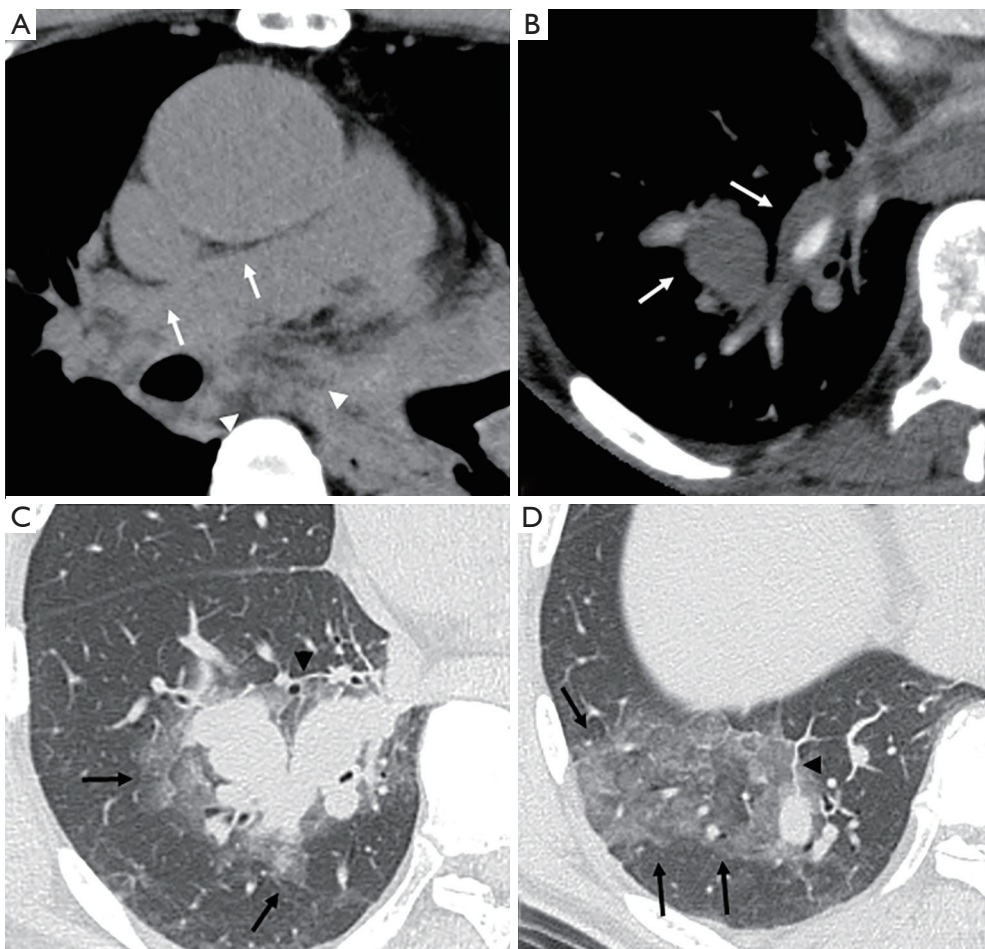


Figure 4 Image for a 58-year-old man with Grade 3 PAPH. (A) Non-enhanced CT showing a higher attenuation area than that of blood along the wall of the right main PA (white arrows) and mediastinal hemorrhage (white arrowheads); (B) CECT showing a thick non-contrast-enhanced area that was a suspected hematoma around the right PA in the right lung field (white arrows); (C,D) CT (lung window setting) showing thickening of the interlobular septum (black arrowheads) and extensive ground-glass opacities beyond the tissue surrounding the PA (black arrows) in the right lung field, indicating blood extending into the alveoli. PAPH, pulmonary artery periaortic hematoma; CT, computed tomography; PA, pulmonary artery; CECT, contrast-enhanced CT.

and between the death and alive groups using the Chi-square test. Univariate and multivariate logistic regression analyses were used to determine the ability of each variable to predict mortality. In the univariate logistic analysis, each variable was examined separately for its association with early death within the first week after onset. Multivariate logistic regression analysis (forced entry) was performed with variables that were significant in the univariate analysis. Two-sided P values ≤ 0.05 were considered statistically significant, and statistical analysis was performed using SPSS for Windows version 22.0 (IBM Japan, Tokyo, Japan).

Results

Clinical characteristics and findings on CT in the PAPH and non-PAPH groups

The patient cohort comprised 78 patients with PAPH [33 men (42.3%) and 45 women (57.7%); mean age (standard deviation): 74.4 years (12.0)] and 238 patients without PAPH [118 men (49.6%) and 120 women (50.4%); mean age (standard deviation): 69.8 years (12.7)] (Table 1).

There was no significant difference between the two groups for sex ($P=0.29$), renal failure ($P=0.24$), smoking

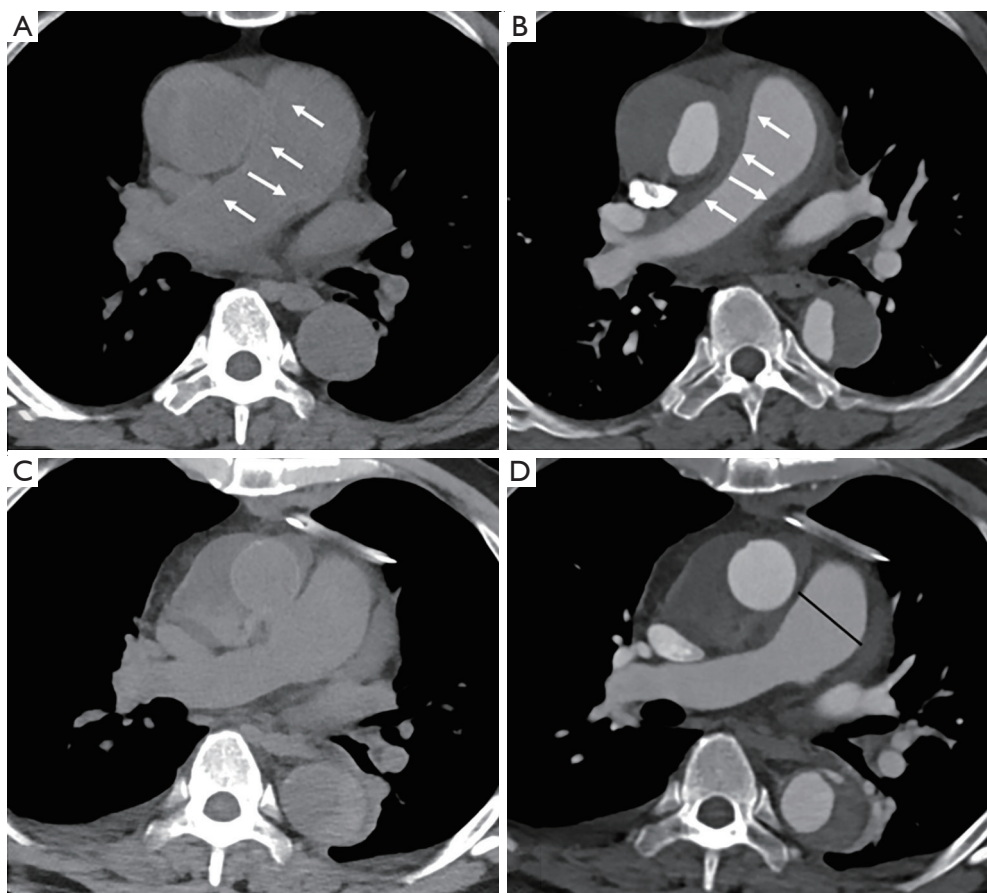


Figure 5 Images for a 51-year-old woman with Grade 1 PAPH. (A) First non-enhanced CT showing a higher attenuation area than that of blood along the wall of the right main PA (white arrows). (B) First CECT showing no contrast enhancement within the area (white arrows). This hematoma induced stenosis of the right main PA. (C,D) Ascending aortic replacement was performed. Follow-up non-enhanced CT and CECT 1 week after the first CT showing disappearance of the hematoma that was due to PAPH, along the wall of the right main PA. Stenosis of the right main PA has improved. We measured the maximum main pulmonary diameter on CECT (black line). PAPH, pulmonary artery periadventitial hematoma; CT, computed tomography; PA, pulmonary artery; CECT, contrast-enhanced CT.

($P=0.19$), anticoagulation therapy ($P=0.88$), inoperable case ($P=0.07$), open false lumen ($P=0.92$), and hemothorax ($P=0.06$). In contrast to the non-PAPH group, the PAPH group was significantly older ($P=0.005$), and had higher rates of early death ($P=0.001$), pericardial hemorrhage ($P<0.001$), and mediastinal hemorrhage ($P<0.001$), and included significantly lower proportions of patients with hypertension ($P=0.02$) and diabetes mellitus ($P=0.03$).

Clinical characteristics and findings on CT in the death and alive groups in the PAPH group

Table 2 shows the clinical characteristics and CT findings of the 78 patients with PAPH in the death and alive groups.

There was no significant difference between the two groups for age ($P=0.15$), sex ($P=0.43$), diabetes mellitus ($P=0.62$), renal failure ($P=0.61$), smoking ($P=0.15$), anticoagulation therapy ($P=0.22$), Grade 2 PAPH ($P=0.13$), open false lumen ($P=0.41$), stenosis of the main PA ($P=0.12$), pericardial hemorrhage ($P=0.51$), and mediastinal hemorrhage ($P=0.08$). In contrast, there was a significant difference between the groups for hypertension ($P=0.009$), inoperable case [$P<0.001$; odds ratio (OR) =12.600, 95% confidence interval (CI): 5.434–29.216], Grade 1 PAPH ($P=0.03$), Grade 3 PAPH (PAPH with pulmonary hemorrhage) ($P<0.001$; OR =17.400, 95% CI: 4.382–69.093), and hemothorax ($P=0.02$; OR =7.625, 95% CI: 1.148–50.636).

Grade 3 *vs.* Grade 1 PAPH was the only comparison that

Table 1 Clinical characteristics and findings on CT in the PAPH and non-PAPH groups (n=316)

Variables	PAPH (n=78)	Non-PAPH (n=238)	P value
Age (years)	74.4±12.0	69.8±12.7	0.005*
Sex (male/female)	33/45	118/120	0.29
Hypertension	34 (43.6)	141 (59.2)	0.02*
Diabetes mellitus	1 (1.3)	20 (8.4)	0.03*
Renal failure	8 (10.3)	15 (6.3)	0.24
Smoking	8 (10.3)	39 (16.4)	0.19
Anticoagulation therapy	20 (25.6)	59 (24.8)	0.88
Inoperable case	20 (25.6)	39 (16.4)	0.07
Death	15 (19.2)	15 (6.3)	0.001*
Open false lumen	50 (64.1)	151 (63.4)	0.92
Pericardial hemorrhage	69 (88.5)	78 (32.8)	<0.001*
Mediastinal hemorrhage	67 (85.9)	43 (18.1)	<0.001*
Hemothorax	5 (6.4)	5 (2.1)	0.06

Data are expressed as mean ± standard deviation or n (%). *, P<0.05. CT, computed tomography; PAPH, pulmonary artery periadventitial hematoma.

Table 2 Clinical characteristics and findings on CT in the death and alive groups in the PAPH group (n=78)

Variables	Death (n=15)	Alive (n=63)	P value	OR (95% CI)
Age (years)	78.2±9.7	73.6±12.3	0.15	–
Sex (male/female)	5/10	28/35	0.43	0.625 (0.191–2.040)
Hypertension	2 (13.3)	32 (50.8)	0.009*	0.149 (0.031–0.715)
Diabetes mellitus	0 (0.0)	1 (1.6)	0.62	1.016 (0.985–1.049)
Renal failure	1 (6.7)	7 (11.1)	0.61	0.571 (0.065–5.033)
Smoking	0 (0.0)	8 (12.7)	0.15	1.145 (1.043–1.259)
Anticoagulation therapy	2 (13.3)	18 (28.6)	0.22	0.385 (0.079–1.878)
Inoperable case	15 (100.0)	5 (7.9)	<0.001*	12.600 (5.434–29.216)
PAPH				
Grade 1	3 (20.0)	32 (50.8)	0.03*	0.242 (0.062–0.942)
Grade 2	3 (20.0)	26 (41.3)	0.13	0.356 (0.091–1.387)
Grade 3	9 (60.0)	5 (7.9)	<0.001*	17.400 (4.382–69.093)
Open false lumen	11 (73.3)	39 (61.9)	0.41	1.692 (0.484–5.920)
Stenosis of the main PA	8 (53.3)	20 (31.7)	0.12	2.457 (0.782–7.719)
Pericardial hemorrhage	14 (93.3)	55 (87.3)	0.51	2.036 (0.235–17.659)
Mediastinal hemorrhage	15 (100.0)	52 (82.5)	0.08	1.212 (1.081–1.357)
Hemothorax	3 (20.0)	2 (3.2)	0.02*	7.625 (1.148–50.636)

Data are expressed as mean ± standard deviation or n (%). *, P<0.05. CT, computed tomography; PAPH, pulmonary artery periadventitial hematoma; PA, pulmonary artery; OR, odds ratio; 95% CI, 95% confidence interval.

Table 3 Multivariate analysis of the factors associated with death (n=78)

Factors	Multivariate		
	OR	95% CI	P value
Hypertension	0.185	0.032–1.055	0.06
PAPH grade			
1	1.000	Ref	
2	1.017	0.176–5.864	0.99
3	12.365	2.218–68.926	0.004*
Hemothorax	4.872	0.238–99.640	0.30

*, P<0.05. PAPH, pulmonary artery periadventitial hematoma; OR, odds ratio; 95% CI, 95% confidence interval; Ref, reference.

Table 4 Main PA diameter between the CT image when PAPH disappeared and the final CT image during the follow-up (n=63)

Variable	CT image when PAPH disappeared (n=63)	Final CT image (n=63)	P value
Major PA diameter (mm)	24.6±7.1	24.3±7.8	0.09

Data are expressed as mean ± standard deviation. PA, pulmonary artery; CT, computed tomography; PAPH, pulmonary artery periadventitial hematoma.

showed a significant difference in the multivariate analysis (OR =12.365, 95% CI: 2.218–68.926; P=0.004). In contrast, there was no significant difference in the multivariate analysis for Grade 2 *vs.* Grade 1 PAPH (OR =1.017, 95% CI: 0.176–5.864; P=0.99). The factor “inoperable case” was excluded from the multivariate analysis because all patients were inoperable in the death group (Table 3).

Changes in PAPH on follow-up CT

All 63 surviving patients in the alive group were followed (mean duration: 31.6±37.7 months; range, 2–159 months) after they underwent the first CT. All hematomas due to PAPH disappeared (mean time to disappearance: 8.6±15.0 weeks; range, 1–72 weeks). There was no significant difference in the maximum PA diameter between the CT image when PAPH disappeared and the final CT image during the follow-up (24.6±7.1 *vs.* 24.3±7.8 mm, respectively; P=0.09) (Table 4).

Discussion

A rare complication of Stanford type A AD is extension of the hematoma along the pulmonary arteries, which is believed to result from rupture through the posterior aspect of the aortic root into the common adventitia of the aorta and PA (1,2,6,9–11) (Figure 6A,6B). Under this condition, extravasated blood from the ascending aorta can extend between the media and adventitia of the main PA and cross the barrier of the pulmonary hilum, which can lead to pulmonary hemorrhage (1,6,7,9,10).

PAPH is a rare complication of Standard type A AD. In 2009, Sueyoshi *et al.* (10) showed that 21 (9.1%) of 232 patients with Stanford type A AD had PAPH. In this study, 78 (24.7%) of 316 patients with Stanford type A AD had PAPH, and in particular, there were many patients with Grade 1 (35 patients, 44.9%) and Grade 2 (29 patients, 37.2%) PAPH. We speculated that the reason for these percentage differences was that recent improvements in CT resolution made it easier to identify small hematomas along the PA in the follow-up imaging.

Notably, a significantly higher rate of pericardial and mediastinal hemorrhage was observed in the PAPH group compared with the non-PAPH group in this study. PAPH indicates high pressure of extravasated blood from an aortic rupture and a large volume of blood. Additionally, the normal pulmonary circulation is a low-pressure system that has approximately one-fifth to one-tenth the flow resistance of the systemic circulation, and the wall of the PA is thinner than that of the aorta (12). As a result, extravasated blood in the wall of the PA may be more likely to penetrate the pericardium and mediastinum compared with the aorta (Figure 6C).

In this study, higher early mortality was observed in the PAPH group compared with the non-PAPH group. Moreover, inoperable case, Grade 3 PAPH (PAPH with pulmonary hemorrhage), and hemothorax were significant risk factors for early death in the univariate analyses in the PAPH group. Hypertension and Grade 1 PAPH were also significant protective factors for early death in the univariate analyses in the PAPH group. Only Grade 3 PAPH (PAPH with pulmonary hemorrhage) was a significant risk factor for early death in the multivariate analyses in the PAPH group.

In a previous study, PAPH with continuous blood extending into the alveoli was a significant risk factor for

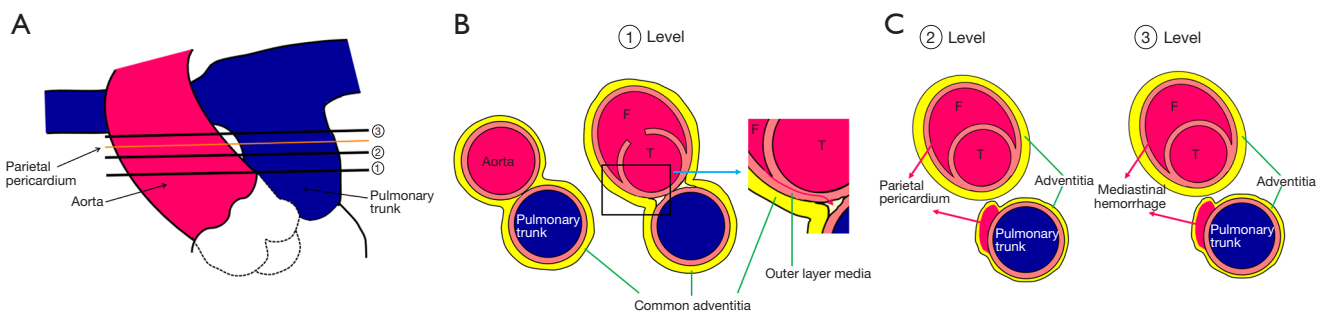


Figure 6 Mechanism of PAPH with Stanford type A AD [reproduced with permission from (10)]. (A) The ascending aorta and pulmonary trunk have a common adventitia at the root of the great vessels (at 1 level). Caudally, the common adventitia becomes the visceral pericardium. (B) At 1 level, when bleeding from the false lumen during aortic dissection ruptures the anterior portion of the outer layer of the media, the hematoma invades between the adventitia and media of the pulmonary artery. (C) Cranially, the common adventitia divides into the adventitia of the aorta and pulmonary artery, respectively. At 2 level, when bleeding from the false lumen of the aortic dissection and hematoma that is due to PAPH ruptures the adventitia, the hematoma penetrates the pericardium. In contrast, at 3 level cranial to the parietal pericardium, when bleeding from the false lumen of the aortic dissection and hematoma that is due to PAPH ruptures the adventitia, the hematoma penetrates the mediastinum. A hematoma due to PAPH in the wall of the PA may be more likely to penetrate the pericardium and mediastinum compared with a hematoma in the aorta because the wall of the PA is thinner than that of the aorta. ①Level 1: area where a common adventitia of the ascending aorta and pulmonary artery is present. ②Level 2: area where a common adventitia of the ascending aorta and pulmonary artery disappeared below the parietal pericardium. ③Level 3: area where a common adventitia of the ascending aorta and pulmonary artery disappeared above the parietal pericardium. F, false lumen; T, true lumen; PAPH, pulmonary artery periaortic hematoma; AD, aortic dissection; PA, pulmonary artery.

death (10). The authors hypothesized that blood extending into the alveoli may cause respiratory failure due to reduced gas exchange (13). The CT finding of hemorrhage into the alveoli also suggested that the pressure of extravasated blood from an aortic rupture was high, with a high blood volume. We also considered that these were the causes of the poor early prognosis, in our study. As Grade 3 PAPH (PAPH with pulmonary hemorrhage) and hemothorax appear to indicate a serious condition, the patients could not undergo operation because of deteriorating general condition. In fact, all nine patients with Grade 3 PAPH who did not undergo surgery died within 1 week, in this study. However, all five patients with Grade 3 PAPH who underwent surgery were alive at the time of writing. This suggests that patients with serious condition due to Grade 3 PAPH (PAPH with pulmonary hemorrhage) may survive if they can undergo surgery, which should be recommended.

To our knowledge, there are few reports about the long-term changes in PAPH. In this study, all hematomas due to PAPH in the 63 surviving patients in the alive group had disappeared (mean time to disappearance: 8.6 ± 15.0 weeks). One previous report showed that aneurysmal dilation of the right PA appeared in patients with PAPH with Stanford type A AD after 11 months (7). The authors considered that

this subsequent aneurysmal change may arise from damage to the wall of the PA as a result of PAPH (7). However, the PA diameter in all surviving patients did not change during the follow-up after PAPH disappeared, in the present study. Morphological changes in PA may be less likely to occur because of the flexibility of the PA wall (12).

Study limitations

This study had several limitations. First, this study included patients with AD from a single institution; therefore, the study lacked an external validation cohort. Second, electrocardiographic gating is needed for assessment of AD. However, many of these patients in this study were emergency patients, and electrocardiographic gating, which takes time to prepare, was often omitted. Third, it is very difficult to distinguish blood extending into the alveoli from cardiogenic edema *vs.* PAPH using only CT findings because the findings for both conditions are similar and overlap (14). In fact, some cases with Grade 3 PAPH (PAPH with pulmonary hemorrhage) might have had blood extending into the alveoli as well as cardiogenic edema. However, the presence of such a combination appears to indicate a more serious condition. Fourth, because patients

in the death group died within 1 week of onset, their medical and life histories, including hypertension, diabetes mellitus, renal failure, smoking status, and coagulation therapy, may not have been fully reviewed. This may have led to a lower proportion of patients in the death group compared with the alive group. Fifth, a cardiovascular surgeon in our hospital decided whether surgery was possible by considering each patient's condition and complications. Moreover, operator-associated influences or surgical technique were not evaluated. Therefore, the data of this study are considered a limited mortality analysis. Finally, because the interval between follow-up CTs varied among the patients, it was difficult to determine exactly when PAPH disappeared in patients with long follow-up CT intervals.

Conclusions

PAPH with Stanford type A ADs not rare. Higher early mortality was observed in the PAPH group compared with the non-PAPH group. Grade 3 PAPH (PAPH with pulmonary hemorrhage) is a significant risk factor for early death.

Acknowledgments

We thank Sushil Dawka, MBBS, MS, from Edanz (<https://jp.edanz.com/ac>) for editing a draft of this manuscript.

Funding: None.

Footnote

Reporting Checklist: The authors have completed the STROBE reporting checklist. Available at <https://jtd.amegroups.com/article/view/10.21037/jtd-23-1914/rc>

Data Sharing Statement: Available at <https://jtd.amegroups.com/article/view/10.21037/jtd-23-1914/dss>

Peer Review File: Available at <https://jtd.amegroups.com/article/view/10.21037/jtd-23-1914/prf>

Conflicts of Interest: All authors have completed the ICMJE uniform disclosure form (available at <https://jtd.amegroups.com/article/view/10.21037/jtd-23-1914/coif>). The authors have no conflicts of interest to declare.

Ethical Statement: The authors are accountable for all

aspects of the work in ensuring that questions related to the accuracy or integrity of any part of the work are appropriately investigated and resolved. The study was conducted in accordance with the Declaration of Helsinki (as revised in 2013). This retrospective study was approved by the institutional review board of Nagasaki University Hospital (No. 23061912), and the institutional review board waived the need for written informed consent because of the retrospective study design.

Open Access Statement: This is an Open Access article distributed in accordance with the Creative Commons Attribution-NonCommercial-NoDerivs 4.0 International License (CC BY-NC-ND 4.0), which permits the non-commercial replication and distribution of the article with the strict proviso that no changes or edits are made and the original work is properly cited (including links to both the formal publication through the relevant DOI and the license). See: <https://creativecommons.org/licenses/by-nc-nd/4.0/>.

References

1. Panicek DM, Ewing DK, Markarian B, et al. Interstitial pulmonary hemorrhage from mediastinal hematoma secondary to aortic rupture. *Radiology* 1987;162:165-6.
2. Buja LM, Ali N, Fletcher RD, et al. Stenosis of the right pulmonary artery: a complication of acute dissecting aneurysm of the ascending aorta. *Am Heart J* 1972;83:89-92.
3. Milne EN, Cyrlak D. Interstitial pulmonary hemorrhage from mediastinal hematoma secondary to aortic rupture. *Radiology* 1987;164:286-7.
4. Castañer E, Andreu M, Gallardo X, et al. CT in nontraumatic acute thoracic aortic disease: typical and atypical features and complications. *Radiographics* 2003;23 Spec No:S93-S110.
5. Colice GL, Lenz J, Schned A. Unilateral hyperlucent lung due to interstitial pulmonary hemorrhage from aortic dissection. *Am J Med* 1989;86:250-2.
6. Sueyoshi E, Sakamoto I, Uetani M, et al. CT findings of ruptured intramural hematoma of the aorta extending along the pulmonary artery. *Cardiovasc Intervent Radiol* 2007;30:321-3.
7. Ratcliffe GE, Kirkpatrick ID. Stanford type A aortic dissection with pulmonary arterial intramural hematoma and pulmonary hemorrhage. *J Cardiovasc Comput Tomogr* 2013;7:141-3.
8. Jinno A, Hirokawa T. Aortic intramural haematoma

- associated with pulmonary artery periadventitial haematoma. *BMJ Case Rep* 2018;2018:bcr2018224853.
9. Roberts WC. Aortic dissection: anatomy, consequences, and causes. *Am Heart J* 1981;101:195-214.
 10. Sueyoshi E, Matsuoka Y, Sakamoto I, et al. CT and clinical features of hemorrhage extending along the pulmonary artery due to ruptured aortic dissection. *Eur Radiol* 2009;19:1166-74.
 11. Neri E, Toscano T, Civeli L, et al. Acute dissecting aneurysm of the ascending thoracic aorta causing obstruction and thrombosis of the right pulmonary artery. *Tex Heart Inst J* 2001;28:149-51.
 12. Townsley MI. Structure and composition of pulmonary arteries, capillaries, and veins. *Compr Physiol* 2012;2:675-709.
 13. Bruzzi JF, Rémy-Jardin M, Delhay D, et al. Multi-detector row CT of hemoptysis. *Radiographics* 2006;26:3-22.
 14. Ledbetter S, Stuk JL, Kaufman JA. Helical (spiral) CT in the evaluation of emergent thoracic aortic syndromes. Traumatic aortic rupture, aortic aneurysm, aortic dissection, intramural hematoma, and penetrating atherosclerotic ulcer. *Radiol Clin North Am* 1999;37:575-89.

Cite this article as: Koike H, Sueyoshi E, Somagawa C, Nagayama H, Toya R. CT findings, prognosis, and follow-up of pulmonary artery periadventitial hematoma with aortic dissection: a retrospective single-center study. *J Thorac Dis* 2024;16(5):3031-3041. doi: 10.21037/jtd-23-1914